



International Journal of Engineering Research and Science & Technology

ISSN : 2319-5991
Vol. 4, No. 3
August 2015



www.ijerst.com

Email: editorijerst@gmail.com or editor@ijerst.com

Research Paper

NUMERICAL MODELING AND ANALYSIS OF ELASTOMER ENCAPSULATED SYSTEM

M Rama Mohan Rao^{1*} and M R S Satyanarayana¹

*Corresponding Author: **M Rama Mohan Rao** ✉ mramohanrao@gmail.com

The aim of this paper is to study the static, vibration, harmonic and shock analysis of Elastomer Encapsulated system. It investigates the performance of elastomer encapsulated system which consists of three different materials Aluminum, ceramic, and elastomer. For nonlinear material system, the curve fit of the experimental investigation with the analytical methods of the standard material models like Ogden, Mooney, Arruda-Boyce, Neo-Hookean, etc., was obtained. It shows that a good fit between the predictions from the analytical models and experimental results. The static analysis is performed for various pressures on the assembly and corresponding peak stress and displacements were observed. The harmonic response of the model of a given frequency range is studied for a given harmonic displacement.

Keywords: Elastomers, Static Analysis, Vibration Analysis, Harmonic Analysis

INTRODUCTION

The ever increasing demands for rubbers and rubber-like materials have attracted the attention of researchers for modeling these materials' behavior under mechanical and geometrical boundary conditions. To characterize the mechanical behavior of these materials, it is a common practice to represent the constitutive equation through a strain energy density function.

Hyperelastic materials are often considered for various industrial applications, due to their remarkable properties of flexibility, deformability and resistance to high deformation levels. Mooney (1940) and Rivlin (1948). Valanis and

Landel (1967) proposed to write the strain energy function into a separable form related to the principal directions. This advance led to the Ogden model (Ogden, 1972, 1982) which is largely used today. The difficulties related to the incompressibility modeling have been treated by Oden (1972, 1982) in the framework of the finite element method.

Many attempts have been made to develop more general hyperelastic models to include different aspects of materials behavior. Rivlin and Saunders (1951) proposed that a strain energy density function is expressible in the form of even powered series of the principal stretches. A

¹ Mechanical Engineering Department, GITAM Institute of technology, GITAM University, Visakhapatnam.

variety of strain energy density functions have been extracted from Rivlin's model. Valanis and Landel (1967) proposed that a strain energy density is sum of independent functions of the principal stretches for incompressible materials. Ogden (1979) proposed that the strain energy function is a series of principal stretches with real positive and negative powers. Kakavas (2000) expressed the strain energy density function in terms of the second and third invariants of the logarithmic strain tensor with three material parameters. Attard (2003) presented the strain energy density is a geometric series of principal stretches containing only even powers. In addition, other constitutive models have been proposed to reflect the nonlinearity in the load-stretch relationships.

The material models formulated in invariants of the strain tensor are based on a series approach in different powers of the first and second basic invariant. Because of the incompressibility of the material, the third basic invariant is constant and, hence, does not contribute to the stored energy. Formulations of the strain energy function based on eigenvalues were presented by Ogden. These models show a good adaptability to the experimental data resulting from the high degree of non-linearity. The examples of these strain energy density functions have been presented in the references (Beatty, 1987, Ehlers and Eipper, 1998, Yeoh, 1990, Yeoh, 1993, Darjani, 1999, El-Lawindy and El-Guiziri, 2000, Boyce and Arruda, 2000, Bradley *et al.*, 2001, Bischoff *et al.*, 2000).

To obtain the optimal efficiency in the series computations, the nonlinear equations of the problem must be set into an appropriate quadratic form. This can be obtained in general by

introducing additional variables and/or differential relations between the variables. In the context of hyperelastic models, strongly nonlinear terms are involved, such as logarithmic or fractional functions.

In the present work, the performance of elastomer encapsulated system which consists of three different materials Aluminum, ceramic, and elastomer by static, vibration and harmonic analysis in which two materials are linear and elastomer is nonlinear. The nonlinear material has been modeled by using uniaxial tension/compression test and the material constants are determined through least-squares-fit procedures using numerical methods and is observed that mooney model is best fitted with less error and those constant are used for analysis under various loading conditions and corresponding results were observed.

CONSTITUTIVE MODEL

The Mooney Rivlin model is a special case of the generalized Rivlin Model. The Mooney Rivlin model has shown potential for accurately predicting the non-linear behavior of isotropic elastomeric materials. Therefore, it has been widely used in many researches and finite element codes as a constitutive model to represent the behavior of hyper-elastic materials. The strain invariants (I_1 , I_2 and I_3) can be expressed in terms of principal stretch ratio or extension ratio as:

$$\begin{aligned} I_1 &= \lambda_1^2 + \lambda_2^2 + \lambda_3^2, \\ I_2 &= \lambda_1^2 \lambda_2^2 + \lambda_2^2 \lambda_3^2 + \lambda_1^2 \lambda_3^2, \\ I_3 &= \lambda_1^2 \lambda_2^2 \lambda_3^2 \end{aligned} \quad \dots(1)$$

where λ_1 , λ_2 , λ_3 are principle stretch ratios (1 + strain).

The general form of strain energy density function is given by

$$W = \sum_{i=0, j=0, k=0}^{\infty} C_{ijk} (I_1 - 3)^i (I_2 - 3)^j (I_3 - 3)^k \quad \dots(2)$$

By considering that rubber is incompressible, i.e., $I_3 = 1$, the above equation reduces to

$$W = \sum_{i=0, j=0}^{\infty} C_{ij} (I_1 - 3)^i (I_2 - 3)^j \quad \dots(3)$$

$$W = \sum_{i=0, j=0}^{\infty} C_{10} (I_1 - 3) + C_{01} (I_2 - 3) \quad \dots(4)$$

This model has two independent parameters. A suitable adjustment of these two parameters was found to be sufficient to capture the stress-strain curve of rubber almost till its peak load. The two parameters of the Mooney-Rivlin model (C_{10} and C_{01}) are evaluated by fitting the parameters to experimental data from uniaxial tensile test.

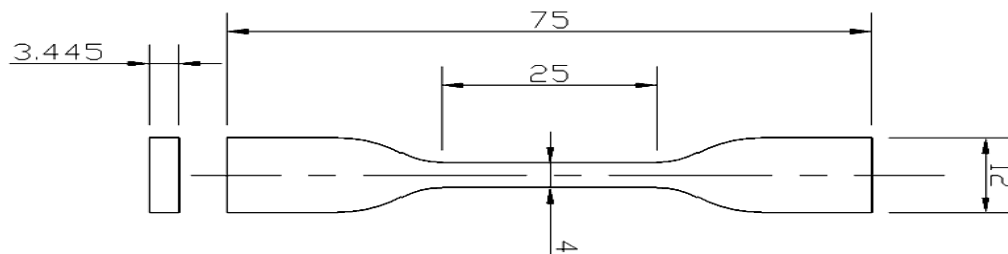
EXPERIMENTAL DETAILS

The standard material models have a set of mathematical forms with different parameters that

are established by using algorithm based curve fitting of experimental data. The strain energy density parameters have been fitted on experimental data from tensile, compression, pure shear. Then, hyperelastic models coefficients were obtained to provide a good fit between the predictions from the model and stress-strain data. The material parameters can be assessed in terms of their ability to match the stress-strain data over a large range of deformations. The fitting results should always be checked in curve fitting approach with the recommended strategies such as using a different model and providing more data points.

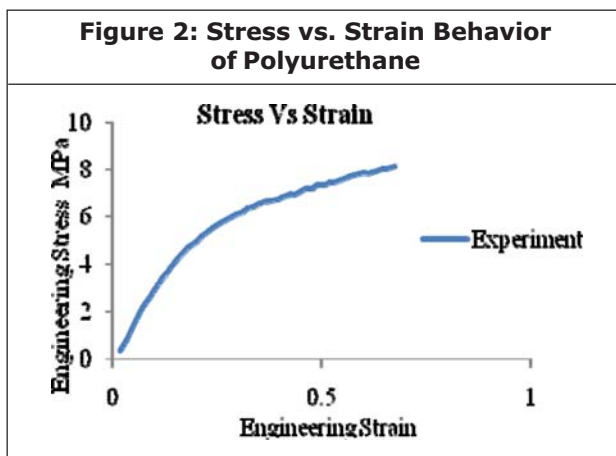
The Experiment was carried out by using Uniaxial Tensile Test Machine shown in Figure 1, having 500 N capacity, it was able to calculate the Tensile Strength, Shear strength and Adhesive Strength. The polyurethane material specimen of 75 mm Gauge Length and Area 13.780 mm² were

Figure 1: Polyurethane Dumble type Specimen & UTM machine



considered based on the guidelines given in ASTM standards. The specimen is fixed at the upper grip and is initially free at the lower grip. During the test, the lower grip moves up to the specimen and clamps it instantaneously at a certain velocity in the downward direction (axial direction).

In the standard UTM machine setup, the distance between the lower and upper grips should be maintained considerably higher than the selected length of the specimen in order to achieve accurate results. Therefore, in this study, mild steel extenders have been connected to the bottom ends of the specimens. The time history of displacement and force were obtained from the UTM Console software. The recorded time histories of displacement were converted into strain histories. Similarly, the force time histories were converted into stress histories. These

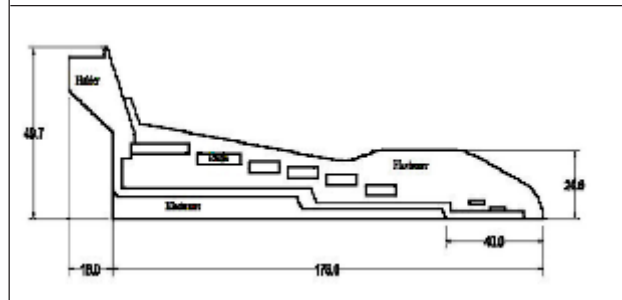


individual time histories were used to obtain the stress-strain relationships for the specimens. As a result, Forces vs. Elongation, Stress vs. Strain, time vs. Load Graphs were obtained, the following graph shows the Stress vs. Strain Graph as shown in Figure 2.

Numerical Modeling

The work mainly involves numerical and analysis

Figure 3: Stress vs. Strain Behavior of Polyurethane



of Elastomer encapsulated system. Finite Element Analysis is carried out with the appropriate forces and boundary conditions are given to the Elastomer Encapsulated system and the static, vibration, harmonic and shock analysis is performed. The Elastomer encapsulated

Table 1: Linear Material Properties of the Elastomer Encapsulated Assembly

Property	Aluminum	PZT-Ceramic
Density (Kg/m3)	2.71E-9	7.60E-9
Young's modulus (N/m2)	71E9	66E9
Poisson's Ratio	0.34	0.34

system line diagram is shown in Figure 3.

Coefficients of Linear and Non-Linear Material Properties of Elastomer Encapsulated System

The linear properties of the materials used in the Elastomer Encapsulated system are tabulated in the Table 1.

$$\sigma = \partial W / \partial \lambda \quad \dots(5)$$

Using incompressibility condition the extension ratios can be expressed as

$$\lambda_1 = \lambda; \lambda_2 = \lambda^{-1/2}; \lambda_3 = \lambda^{-1/2} \quad \dots(6)$$

Using (5) and (6)

$$\sigma_{num} = (2\lambda - 2/\lambda^2) [C_{10} + C_{01}/\lambda] \quad \dots (7)$$

By least square fitting method, residue

between λ_{exp} and λ_{num} for different values of λ is given by

$$R = \sum (\sigma_{exp} - \sigma_{num})^2 \quad \dots(8)$$

The non-linear material properties of the Elastomer is also obtained by the curve fit of the experimental data with the standard material models like Ogden, Mooney, Arruda-Boyce, Neo-Hookean, etc., using numerical method for evaluation of coefficients and shown in Figure 4.

The evaluated coefficients using numerical method best fitted with Mooney material model with less error is given in the following Table.2. These co-efficients were used as material properties of polyurethane material.

STATIC ANALYSIS

Static analysis represents the most basic type of analysis. In this analysis the Elastomer Encapsulated assembly was subjected to a uniform pressure on outer elastomer of 1.5, 3.0, 4.5, 6.0 Mpa pressures and corresponding responses like displacement, von-misses stress and contact stresses were predicted. Path plots of von-misses stress and displacements of middle planes of aluminum holder, Ceramic rings and Polyurethane material are given in the Figures 5 to 10.

MODAL ANALYSIS

Modal analysis is the process of determining the

Figure 4: Curve fit for Elastomer Material to Mooney Model

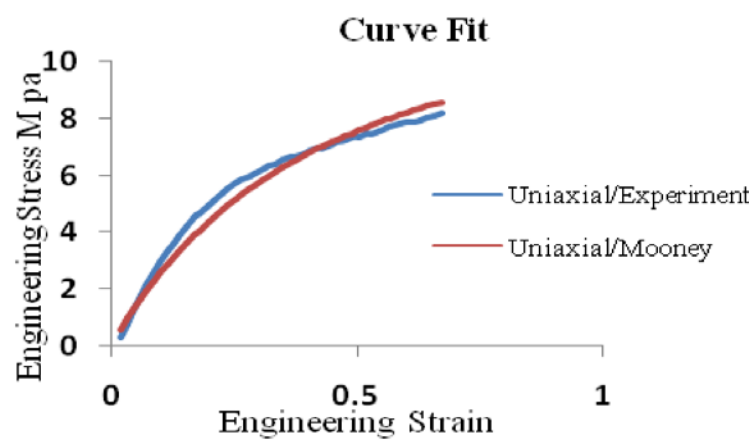


Table 2: Evaluated Co-efficients for Elastomer Material Model

	Neo-Hookean	Mooney-Rivlin(2)	Mooney-Rivlin(3)	Signiorini
C_{10} (Mpa)	3.86814	0.497037	2.06078	2.21232
C_{01} (Mpa)	-	4.62338	2.48514	2.27903
C_{11} (Mpa)	0	-	-	-
C_{20} (Mpa)	-	-	-	0
Error	1.54756	0.730895	0.905639	0.940979

Figure 5: Path Plots For Aluminum Holder Middle Plane Distance From Fixed End To Free End Vs Vonmises Stress

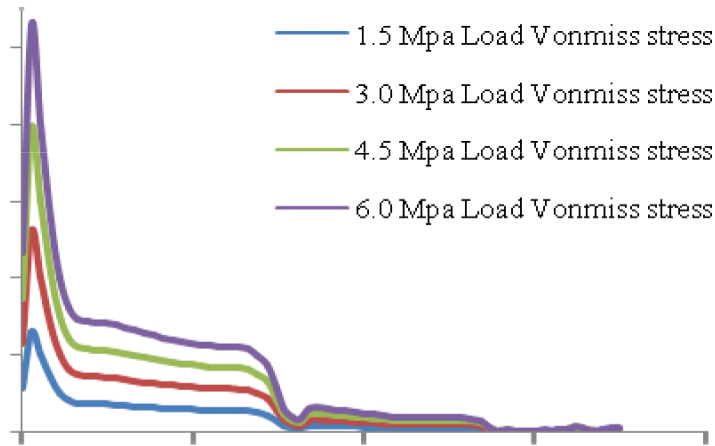


Figure 6: Path Plots For Aluminum Holder Middle Plane Distance From Fixed End To Free End Vs Displacement

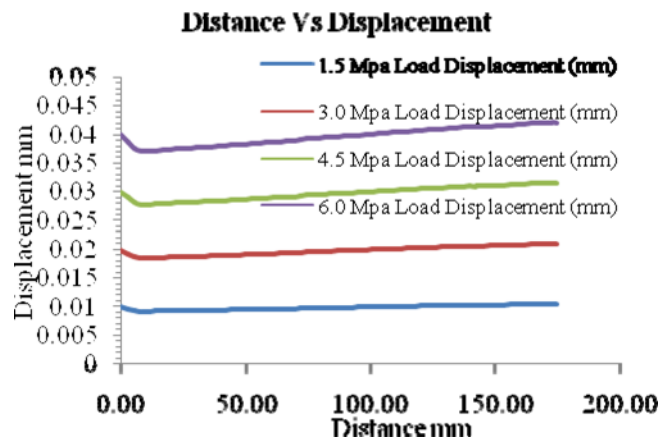


Figure 7: Path Plots For First Ceramic Ring Middle Plane Distance From Fixed Vs Vonmises Stress

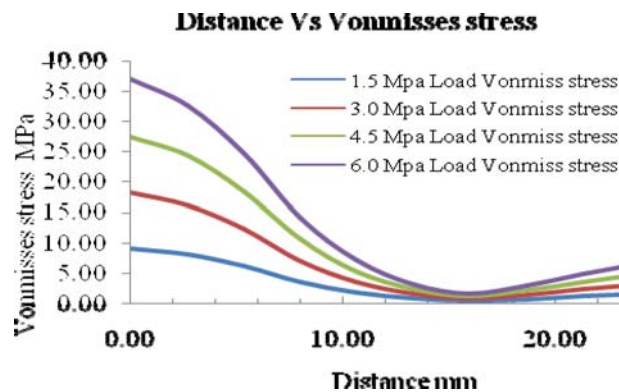


Figure 8: Path Plots For First Ceramic Ring Middle Plane Distance From Fixed Vs Displacement

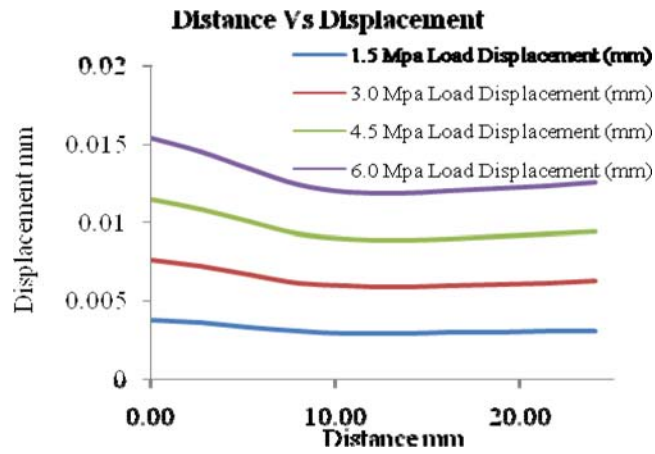


Figure 9: Path Plots For Polyurethane Middle Plane Distance From Fixed End To Free End Vs Vonmises Stress

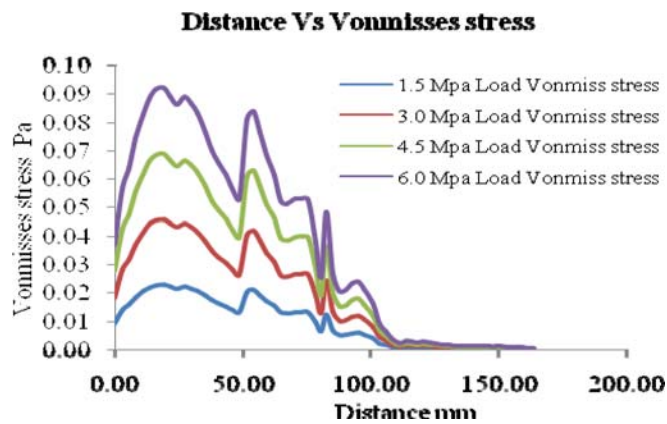
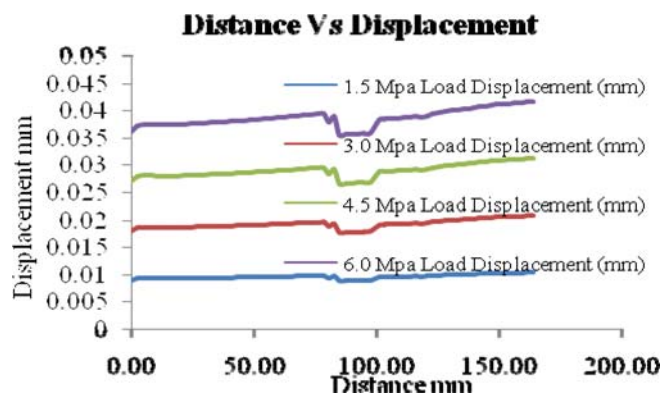
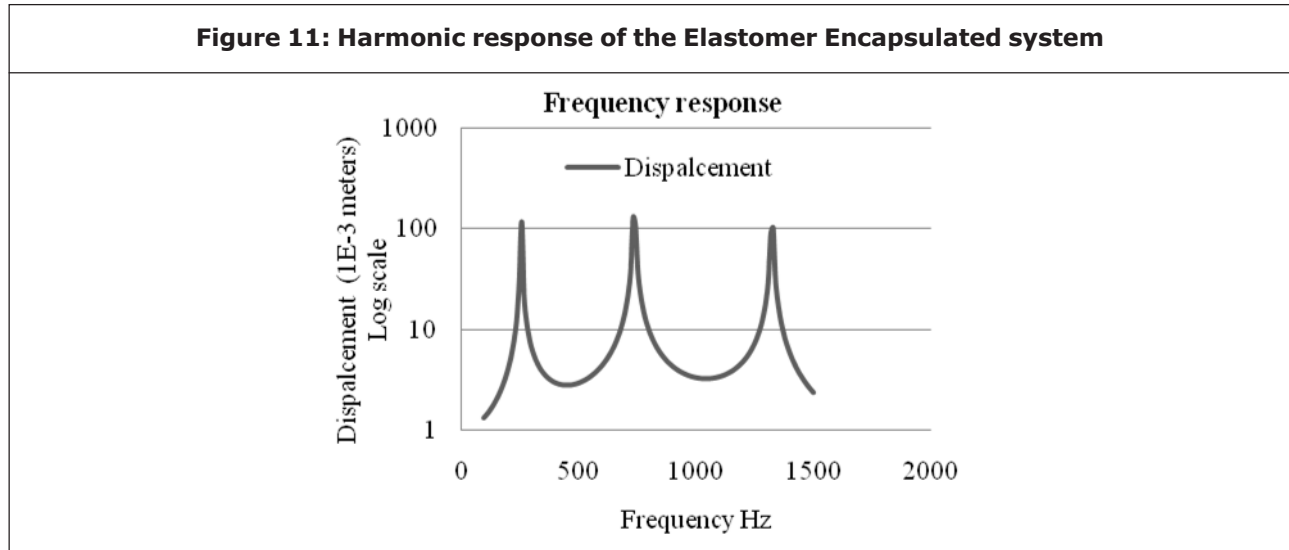


Figure 10: Path Plots For Polyurethane Middle Plane Distance From Fixed End To Free End Vs Displacement



Mode shape	1	2	3	4	5	6	7
Frequency (Hz)	259	567.8	692	739	969.8	1199	1324



inherent dynamic characteristics of a system in forms of natural frequencies, damping factors and mode shapes, and using them to formulate a mathematical model for its dynamic behavior. The natural modes of vibration are inherent to a dynamic system and are determined completely by its physical properties (mass, stiffness, damping) and their spatial distributions. Each mode is described in terms of its modal parameters: natural frequency, the modal damping factor and characteristic displacement pattern, namely mode shape. Each corresponds to a natural frequency. The degree of participation of each natural mode in the overall vibration is determined both by properties of the excitation source(s) and by the mode shapes of the system. The natural frequencies of the Elastomer Encapsulated system are shown in the following Table 3.

FREQUENCY RESPONSE ANALYSIS

Frequency response is the quantitative measure of the output spectrum of a system or device in response to a stimulus, and is used to characterise the dynamics of the system. It is a measure of magnitude and phase of the output as a function of frequency, in comparison to the input. In simplest terms, if a sine wave is injected into a system at a given frequency, a linear/nonlinear system will respond at that same frequency with a certain magnitude and a certain phase angle relative to the input. In many practical applications, components are dynamically excited. Based on operating frequency range (10 Hz to 1500 Hz) of Elastomer Encapsulated system, the harmonic analysis is done by applying fixed displacement of 1 mm at Aluminum holder frequencies from 10 Hz to 1500 Hz. This analysis is to identify the resonant frequencies,

hence limits of displacement can be given. The results are plotted as frequency vs. displacement graphs given in the Figure.11

CONCLUSION

An approach was made to model and discretize the elastomer encapsulated assembly with FEA software. The Maximum stresses and deformation locations are obtained for each part of the system for 1.5, 3.0, 4.5, 6.0 Mpa pressure on outer elastomer. The stresses and deformations of path plots for all parts are increases with the applied pressure and it is observed that the stresses are decreases and deformations are increases from fixed end to free end in mid plane. Through the detailed finite element analysis the maximum stresses and deformations were observed to be on the ceramic rings and elastomers. The Natural frequencies of the assembly were predicted. The harmonic response of the system at the peak frequencies in the range 10 Hz to 1500 Hz is plotted.

REFERENCES

1. Attard M M (2003), "Finite strain isotropic hyperelasticity", *Int. J. Solids Struct.*, Vol. 40, pp. 4353–4378.
2. Beatty M F (1987), "Topics in finite elasticity: hyperelasticity of rubber, elastomers and biological tissues with examples", *Appl.Mech. Rev.*, Vol. 40, pp. 1699–1734.
3. Bischoff J E, Arruda E M, Gosh K (2000), "A new constitutive model for the compressibility of elastomers at finite deformations", *Rubber Chem. Technol.*, Vol. 74, pp. 541–559.
4. Boyce M C and Arruda E M (2000), "Constitutive models of rubber elasticity", *Rubber Chem. Technol.*, Vol. 73, pp. 504–523.
5. Bradley G L, Chang P C and Mckenna G B (2001), "Rubber modeling using uniaxial test data", *J. Appl. Poly. Sci.*, Vol. 81, pp. 837–848.
6. Darijani H R, Naghdabadi Lambert-Diani J, Rey C (1999), "New phenomenological behavior laws for rubbers and thermoplastic elastomers", *Eur. J. Mech.A/Solids*, Vol. 18, pp. 1027–1043.
7. Ehlers W and Eipper G. (1998), "The simple tension problem at large volumetric strains computed from finite hyperelastic material laws", *Acta Mech.*, Vol. 130, pp. 17–27.
8. El-Lawindy A M Y and El-Guiziri S B (2000), "Strain energy density of carbon-black-loaded rubber vulcanizates", *J. Phys. D: Appl.Phys.*, Vol. 33, pp. 1894–1901.
9. Kakavas P A (2000), "A new development of the strain energy function for hyperelastic materials using a logarithmic strain approach", *J. Appl. Poly. Sci.*, Vol. 77, pp. 660–672.
10. Mooney M (1940), "A theory of large elastic deformations", *J Appl Mech.*, Vol. 11, pp. 582–592.
11. Oden J (1972), *Finite elements of non-linear continua*, McGraw-Hill, New York
12. Ogden R (1972), "Large deformation isotropic elastic—on the correlation of theory and experiment for incompressible rubberlike solids", In: Proceedings of the Royal Society A, Vol. 326, pp. 565–584.
13. Ogden R (1982), "Elastic deformation of rubber-like solids", In: Hopkins H G and Sewell M J (eds.), *Mechanics of solids*, The Rondey Hill 60th Anniversary Volume. Pergamon, Oxford.

14. Oden J and Kikuchi N (1982), "Finite element methods for constrained problems in elasticity", *Int J Numer Methods Eng.*, Vol. 18, pp. 701–725.
15. Ogden R W (1979), "Biaxial deformation of rubber-like solids: comparison of theory and experiment", *J. Phys. D: Appl. Phys.*, Vol. 12, pp.1463–1472.
16. Rivlin R (1948), "Large elastic deformations of isotropic materials.IV. Further developments of the general theory", *Philos Trans R SocLond Ser A*, Vol. 241, pp. 379–397.
17. Rivlin R S and Saunders D W (1951), "Large elastic deformations of isotropic materials VII, experiments on the deformation of rubber", *Phil. Trans. R. Soc. A*, Vol. 243, pp. 251–288.
18. Valanis K and Landel R (1967), "The strain-energy function of a hyperelastic material in terms of the extension ratios", *J Appl Phys.*, Vol. 38, pp. 2997–3002.
19. Yeoh O H (1990), "Characterization of elastic properties of carbon black filled rubber vulcanizates", *Rubber Chem. Technol.*, Vol. 63, pp. 792–805.
20. Yeoh O H (1993), "Some forms of the strain energy function for rubber", *Rubber Chem. Technol.*, Vol. 66, pp. 754–771.

NOMENCLATURE

I_1, I_2, I_3	Strain invariants
$\lambda_1, \lambda_2, \lambda_3$	Principal stretch ratios (1+principal strains)
W	Strain energy density N-m
$C_{10}, C_{01}, C_{11}, C_{20}$	Co-efficient of non linear material models Mpa
Hz	Frequency number of rotations per second
g	Acceleration due to gravity (m/sec ²)
σ	Stress N/mm ²
σ_{exp}	Experimental stress N/mm ²
σ_{num}	Calculated stress from numerical values N/mm ²
R	Difference of experimental and numerical stress



International Journal of Engineering Research and Science & Technology

Hyderabad, INDIA. Ph: +91-09441351700, 09059645577

E-mail: editorijerst@gmail.com or editor@ijerst.com

Website: www.ijerst.com

